

RESEARCH ARTICLE

Deletion of estrogen receptor α in skeletal muscle results in impaired contractility in female mice

Brittany C. Collins,¹ Tara L. Mader,¹ Christine A. Cabelka,¹ Melissa R. Iñigo,² Espen E. Spangenburg,² and Dawn A. Lowe¹

¹Divisions of Rehabilitation Science and Physical Therapy, Department of Rehabilitation Medicine, Medical School, University of Minnesota, Minneapolis, Minnesota; and ²East Carolina Diabetes and Obesity Institute, Department of Physiology, Brody School of Medicine, East Carolina University, Greenville, North Carolina

Submitted 20 September 2017; accepted in final form 17 January 2018

Collins BC, Mader TL, Cabelka CA, Iñigo MR, Spangenburg EE, Lowe DA. Deletion of estrogen receptor α in skeletal muscle results in impaired contractility in female mice. *J Appl Physiol* 124: 980–992, 2018. First published January 18, 2018; doi:10.1152/jappphysiol.00864.2017.—Estradiol deficiency in females can result in skeletal muscle strength loss, and treatment with estradiol mitigates the loss. There are three primary estrogen receptors (ERs), and estradiol elicits effects through these receptors in various tissues. Ubiquitous ER α -knockout mice exhibit numerous biological disorders, but little is known regarding the specific role of ER α in skeletal muscle contractile function. The purpose of this study was to determine the impact of skeletal muscle-specific ER α deletion on contractile function, hypothesizing that ER α is a main receptor through which estradiol affects muscle strength in females. Deletion of ER α specifically in skeletal muscle (skmER α KO) did not affect body mass compared with wild-type littermates (skmER α WT) until 26 wk of age, at which time body mass of skmER α KO mice began to increase disproportionately. Overall, skmER α KO mice had low strength demonstrated in multiple muscles and by several contractile parameters. Isolated extensor digitorum longus muscles from skmER α KO mice produced 16% less eccentric and 16–26% less submaximal and maximal isometric force, and isolated soleus muscles were more fatigable, with impaired force recovery relative to skmER α WT mice. In vivo maximal torque productions by plantarflexors and dorsiflexors were 16% and 12% lower in skmER α KO than skmER α WT mice, and skmER α KO muscles had low phosphorylation of myosin regulatory light chain. Plantarflexors also generated 21–32% less power, submaximal isometric and peak concentric torques. Data support the hypothesis that ablation of ER α in skeletal muscle results in muscle weakness, suggesting that the beneficial effects of estradiol on muscle strength are receptor mediated through ER α .

NEW & NOTEWORTHY We comprehensively measured in vitro and in vivo skeletal muscle contractility in female estrogen receptor α (ER α) skeletal muscle-specific knockout mice and report that force generation is impaired across multiple parameters. These results support the hypothesis that a primary mechanism through which estradiol elicits its effects on strength is mediated by ER α . Evidence is presented that estradiol signaling through ER α appears to modulate force at the molecular level via posttranslational modifications of myosin regulatory light chain.

estradiol; hormone receptor; muscle physiology; power; strength

INTRODUCTION

Aging is associated with decreased skeletal muscle strength, which contributes to the inability to carry out activities of daily living (see, e.g., Ref. 14). Both men and women experience strength loss with aging, but at differing rates (7, 9, 22, 23, 56). The sex difference is most robust at the time women experience menopause (see, e.g., Ref. 56), coinciding with a sharp decline in the sex hormone estradiol. There are reports of enhanced muscle strength in postmenopausal women on hormone therapy (HT) (20, 56–58, 64), but those results are not consistent with all other studies. To address discrepancies in the literature, a meta-analysis of 23 papers comparing strength in postmenopausal women on estrogen-based HT vs. those not on HT was conducted and concluded an overall positive effect of HT on muscle strength (26).

Similarly, ovarian hormone deficiency in adult female mice results in decrements in skeletal muscle force generation, and the decrements are reversed by estradiol treatment (26, 35, 46, 47, 65). Moran et al. (46, 47) showed that force generation deficits with ovarian hormone deficiency resulted from impaired muscle quality; specifically, there was less strongly bound (force generating) myosin to actin during contraction, which was reversed with estradiol treatment. Similarly, Qaisar et al. (58) showed that HT in postmenopausal twins improved fiber force generating capacity, without affecting fiber size, compared with that of twin pairs not on HT. Phosphorylation of the regulatory light chain of myosin is estradiol sensitive (16, 39, 44), thus providing additional evidence for estradiol's critical role in modulating myosin-actin interactions in skeletal muscle, ultimately impacting how muscle contracts and produces force. Moreover, studies on both women and female rodents show that estradiol has regulatory roles in energy metabolism and mitochondrial function, which can also affect muscle contractility (13, 21, 32, 37, 49, 50, 61, 62). What is less clear is whether estradiol mediates its effects on contractility through estrogen receptors (ERs) or via a non-receptor-mediated mechanism.

The primary action of estradiol in reproductive tissues is regulated by ERs through classical ligand-activated transcription factor mechanisms. In this process, two ERs dimerize upon activation by estradiol, translocate to the nucleus, bind to estrogen response elements in target gene promoters, and elicit a transcriptional response (15, 36). However in nonreproductive tissues, ERs can elicit responses with nonclassical mech-

Address for reprint requests and other correspondence: D. A. Lowe, MMC 388, 420 Delaware St. SE, Minneapolis, MN 55455 (e-mail: lowex017@umn.edu).

animals (15) as well as classical ligand-activated mechanisms, demonstrating the need to determine estradiol mechanisms in specific tissues, such as skeletal muscle.

To date, there are three recognized ERs: estrogen receptor alpha (ER α), estrogen receptor beta (ER β), and G protein-coupled receptor (GPER). Tissue-specific receptor content and actions through which estradiol elicits effects, particularly in nonreproductive tissues, are being realized. For example, estradiol's role in metabolism specifically through ER α has been demonstrated in transgenic mice lacking ER α (42, 60, 70). Whole body deletion of ER α in mice affects multiple metabolic tissues (i.e., pancreas, skeletal muscle, liver, and adipose tissue), resulting in hyperinsulinemia, insulin resistance (11, 42), impaired oxidative metabolism (60), increased inflammation (60), impaired glucose tolerance (4, 5, 11, 42), decreased physical activity (54), and increased fat and body masses (24, 29, 60). Thus, ubiquitous knockout of ER α results in a phenotype similar to that of metabolic syndrome (30, 43, 60). This creates a situation in which it is difficult to directly assess skeletal muscle autonomous effects of ER α because skeletal muscle contractility can be impaired secondarily to reduced physical activity, obesity, and metabolic disorders. Therefore, analysis of an ER α skeletal muscle-specific knockout mouse is critical to determination of the skeletal muscle autonomous effects of ER α deficiency.

A skeletal muscle-specific ER α -knockout mouse developed by Ribas and coworkers was reported to have metabolic deficits similar to those observed in whole body ER α -knockout mice, including impaired glucose tolerance, insulin resistance, and impaired fatty acid oxidation (59). Modest fatigability of the soleus muscle was suggested, but thorough assessment of skeletal muscle contractility was not presented, such that the impact of ER α deficiency on muscle contractile function remains unclear. The purpose of the present study was to employ a mouse model that is deficient in ER α specifically in the skeletal muscle fibers to comprehensively measure contractile properties of several hindlimb skeletal muscles. This model allows us to overcome a number of experimental limitations that have previously hampered accurate interpretation of the role ER α plays in influencing skeletal muscle. We hypothesize that contractility will be impaired because ER α is the primary mode through which estradiol affects skeletal muscle.

METHODS

Generation of Transgenic Mice

Generation of ER α floxed mice has been previously described (19, 31). Human skeletal actin cre (HSAcre) mice were obtained (strain 006149 originated from The Jackson Laboratory, Bar Harbor, ME). Human skeletal actin is the promoter of choice to drive gene expression specifically in skeletal muscle (45). To generate a skeletal muscle-specific knockout of ER α , homozygote ER α floxed females were crossed with male HSAcre mice. Heterozygote ER α floxed males that were HSAcre positive were subsequently crossed with homozygote ER α floxed females to generate homozygote ER α floxed mice positive for HSAcre (skmER α KO) and homozygote ER α floxed mice negative for HSAcre (skmER α WT). Genotype was determined by PCR with primers (F: GACTCGCTACTGTGCCGTGTGC; R: CTTCCCTGGCATTACCACTTCTCCT) for ER α floxed and HSAcre (3, 45).

Female mice were used in experiments at 15–24 wk of age. The exception was the use of 15 mice (8 skmER α WT and 7 skmER α KO)

aged 34–35 wk for body mass and composition assessments. One group of mice was used for measuring wheel running activity. A second group of mice was used for measuring cage activities followed by soleus and extensor digitorum longus (EDL) muscle contractility and related soleus muscle outcomes. A third group of mice was used for in vivo plantarflexor measurements and a fourth group of mice for in vivo dorsiflexor measurements. Mouse numbers for each experiment (each group of mice) are given in figures and tables.

Mice of the same age were housed in groups of three to five and had access to phytoestrogen-free food (Harlan-Teklad; no. 2019) and water ad libitum. The room was maintained on a 14:10-h light-dark cycle. All animal procedures were reviewed and approved by the Institutional Animal Care and Use Committees at the University of Minnesota and were in accordance with guidelines put forth by the American Physiological Society.

Verification and Specificity of Skeletal Muscle ER α Knockout

qRT-PCR. RNA from mouse tissues was isolated with TRIzol reagent according to the manufacturer's instructions. RNA was resuspended in 20 μ l of ultrapure distilled water (DNase, RNase free; Invitrogen by Life Technologies), and concentration and purity were assessed by spectrophotometry. Only samples with a ratio of spectrophotometric absorbance at 260 nm to that at 280 nm in the range of 1.9–2.1 were used for cDNA synthesis. cDNA was synthesized from 1 μ g of RNA according to directions in the SuperScript IV VIL0 cDNA synthesis kit (catalog no. 11756050; ThermoFisher, Waltham, MA). Relative quantitation of the ER α transcript was determined with TaqMan probes (ThermoFisher) for ESR1 (Mm00433149_m1) and housekeeping gene 18S rRNA (catalog no. 4333760F). Efficiencies for the housekeeping gene (18S) and the target gene ESR1 were both acceptable (slope \leq -3.3). The expression of the reference gene did not vary significantly between the genotypes. Reactions with no reverse transcription and no template were added as negative controls.

Western blot. Freshly dissected skeletal muscle and nonmuscle tissues from female skmER α WT and skmER α KO mice were soaked in ice-cold PBS and chopped over ice. Chopped tissues were further homogenized in NP-40 lysis buffer containing protease inhibitor tablet (catalog no. 11836170001; Roche Diagnostics, Indianapolis, IN) and phosphatase inhibitor II and III cocktails (catalog nos. P5726 and P0044; Sigma-Aldrich, St. Louis, MO) with a bullet blender according to the manufacturer's instruction (Midwest Scientific, St. Louis, MO). Homogenates were centrifuged at 664 g for 10 min at 4°C to remove connective tissue. The supernatant was collected and centrifuged at 800 g for 5 min at 4°C to remove myofilaments. Supernatant was collected, and Bradford protein assay was completed to determine protein concentrations for loading onto gels. Loading buffer was added to protein lysates (60 μ g), heated for 5 min at 95°C, loaded on 10% SDS-PAGE gels, and run at 100 V for 30 min and then 70 V for 2 h. Proteins were transferred to nitrocellulose membranes and probed for ER α (1:800, MC-20, sc-542; Santa Cruz Biotechnology, Dallas, TX) and GAPDH (1:10,000, G9545; Sigma Aldrich) overnight at 4°C. Membranes were washed, incubated with a secondary antibody for 1 h, washed, and then scanned with the Odyssey Infrared Imaging System (LI-COR Biosciences, Lincoln, NE).

Characterization of Transgenic Mice

Vaginal cytology. The estrous cycle in female mice is 4–5 days long (51). Therefore, vaginal swabs were taken from a subgroup of female skmER α WT and skmER α KO mice for 5 consecutive days to verify that mice were cycling normally. In brief, a cotton swab was soaked in sterile PBS and inserted in the vaginal canal. Cells were smeared onto a glass microscope slide. Cells were stained with hematoxylin for 5 min and washed in tap water. Estrous cycle was determined by the type of cell present (51). No attempt was made to conduct subsequent physiological muscle testing or to kill the mice at

any given phase of the estrous cycle; both skmER α WT and skmER α KO mice were studied and killed at random phases of estrus.

Body composition. An Echo MRI 3-in-1 (Echo Medical System, Houston, TX) was used to measure total lean and fat masses in conscious mice.

Physical Activities

Cage activities. Physical activities of individual mice were measured over a 24-h period with open-field activity chambers (Med Associates, St. Albans, VT). Immediately before measurement of activity, each mouse was placed in a mock chamber for a 24-h familiarization period. Activity data was acquired with Activity Monitor version 5 software (Med Associates) with a box size set to "3" (4.8 cm²). Activity counts and box size rationale have been previously described (27). Food intake for each mouse was measured during the 24-h activity period.

Wheel running. Voluntary running wheel distance was measured in a separate group of female mice ($n = 11$ and 10 for skmER α WT and skmER α KO, respectively) to avoid any possible training effect on subsequent muscle contractile measurements. Mice were individually housed in wheel running cages (Mouse Single Activity Wheel Chamber model 80820; Lafayette Instrument, Lafayette, IN) with wheel diameter of 12.7 cm. Revolutions were counted via optical sensor connected to a USB interface for 14 consecutive days. Data was recorded via Activity Wheel Monitor Software model 86065. Data reported are only those from days 8–14 in order to avoid the variability that occurs during the first week of wheel running because of the mice learning and becoming familiar with the wheel.

Skeletal Muscle Physiology

In vitro soleus and extensor digitorum longus muscle contractile functions. Mice were weighed and anesthetized by an intraperitoneal injection of pentobarbital sodium (100 mg/kg body mass), with supplemental doses given as required. The soleus muscle from one hindlimb and the EDL muscle from the contralateral hindlimb of each mouse were studied to determine muscle contractile function. The isolated muscle preparation used was similar to that described previously (25, 27, 48). Briefly, after a muscle was excised, it was mounted in a 1.2-ml bath assembly filled with Krebs-Ringer bicarbonate buffer maintained at 25°C and the proximal tendon was attached to a dual-mode muscle lever system (300B-LR; Aurora Scientific, Aurora, ON, Canada). Muscles were set to their anatomic optimal length (L_0) and measured with digital calipers. Muscles remained quiescent in the bath for 10 min, and then a protocol for testing contractile function began. First, muscles underwent three to eight isometric tetanic contractions (400-ms stimulation at 120 Hz for soleus muscles and 200 ms at 180 Hz for EDL muscles) with 3 min of rest between contractions until maximal isometric tetanic force had plateaued. Three minutes later, peak twitch force was elicited by stimulating the muscle with a 0.5-ms pulse at 150 V, followed by a second twitch 30 s later. A maximal isometric tetanic contraction was again performed 30 s later. After 3 min of rest, a second maximal tetanic contraction was elicited, and at peak force a sinusoidal length oscillation of 0.01% L_0 at 500 Hz was imposed to determine active stiffness (48). Then a series of 10 isometric contractions was performed at increasing frequencies: 5, 10, 15, 20, 25, 30, 40, 50, 70, and 110 Hz for soleus muscles and 10, 20, 25, 30, 40, 50, 60, 80, 120, and 160 Hz for EDL muscles. Contractions were separated by 3 min of rest. Muscles were then measured for maximal concentric force elicited by passively lengthening the muscle to 110% L_0 over 3 s and stimulating tetanically for 133 ms as the muscle was shortened to 90% L_0 . Three minutes later, eccentric force was elicited by passively shortening the muscle to 90% L_0 and then stimulating tetanically as it lengthened to 110% L_0 at 1.5 L_0/s . In a subset of soleus and EDL muscles, fatigability was assessed 3 min after the eccentric contraction. Soleus muscles were stimulated for 1,000 ms at 40 Hz every 5 s for 5 min

(27). EDL muscles underwent 200-ms stimulations at 60 Hz every 10 s for 5 min. Recovery from fatigue was assessed by eliciting one peak isometric tetanic contraction immediately after the fatigue protocol and every 5 min for 20 min thereafter. Additional parameters measured from isometric twitch and tetanic contractions include time to peak twitch, twitch one-half relaxation time, maximal rate of isometric tetanic force development (+dP/dt), and maximal rate of relaxation (−dP/dt).

After contractility testing, each soleus and EDL muscle was removed from the bath, trimmed at the myotendinous junctions, blotted, weighed, snap-frozen in liquid nitrogen, and stored at −80°C until further analysis. Contralateral soleus and EDL muscles were dissected and mounted in OCT; tibialis anterior (TA), gastrocnemius, and quadriceps muscles, visceral and subcutaneous fat pads, and uterus were collected from each mouse and stored at −80°C until further analysis. Mice were euthanized with an overdose of pentobarbital sodium (200 mg/kg) after all tissues were collected.

In vivo plantarflexor muscle function. While several measures of contractility can be measured in isolated muscles, only small muscles such as soleus or EDL are viable for extensive testing because of oxygen diffusion limitations (6). Testing of larger muscle groups such as the ankle plantarflexors and dorsiflexors are important because such groups of muscles are more functionally relevant, e.g., for ambulation. Thus, we next measured contractility of those muscle groups in vivo. Mice were anesthetized via isoflurane inhalant (1%) with oxygen at a flow rate of 125 ml/min and maintained under anesthesia for the duration of testing on a 37°C heating pad. We narrowed these experiments to females only because minimal sex \times genotype interactions were determined for soleus and EDL muscle contractility measures. As previously described in detail, for plantarflexor testing the peroneal branch of the sciatic nerve was severed to avoid recruitment of antagonistic dorsiflexor muscles (1, 12). The ankle joint was then positioned such that the foot was perpendicular to the tibia (defined as neutral position 0°), and the knee was stabilized by a clamp to inhibit movement of the lower limb. The foot was secured to a footplate that was attached to the shaft of a servomotor (300B-LR; Aurora Scientific). Passive torque about the ankle was measured by passively moving the foot −20°, −15°, −10°, −5°, 0°, 5°, 10°, 15°, and 20° in randomized order. Contraction of the plantarflexor muscle group (gastrocnemius, soleus, and plantaris) was elicited via stimulation of the sciatic nerve through platinum percutaneous electrodes attached to a stimulator (E2-12 and S48; Grass Telefactor, Warwick, RI). Peak isometric torque about the axis of the ankle was determined by stimulating the nerve for 200 ms with 0.1-ms square-wave pulses at a frequency of 300 Hz and voltage increasing from 4 to 12 V until maximum torque was achieved. Peak isometric torque at nine ankle angles was measured by stimulating at 5° intervals from 20° plantarflexion to 20° dorsiflexion (1). Torque as a function of stimulation frequency was measured at 10–300 Hz. Peak concentric torque was measured by passively moving the foot from 0 to 19° of dorsiflexion followed by 38° of plantarflexion at an angular velocity of 2°/ms during stimulation. Peak eccentric torque was measured by passively moving the foot from 0 to 19° of plantarflexion followed by 38° dorsiflexion at an angular velocity of 2°/ms during stimulation. To assess the relationship between torque and velocity, a series of concentric contractions were performed at set velocities from 0 to 1,200°/s. Power was calculated by multiplying the torque generated at each velocity by the velocity in radians per second.

In vivo dorsiflexor muscle function. In brief, a separate cohort of mice were anesthetized and positioned on the in vivo apparatus similarly as described in *In vivo plantarflexor muscle function*. Muscle function of the dorsiflexor muscles (TA, EDL, and extensor hallucis longus) was assessed by stimulation through platinum percutaneous electrodes attached to a stimulator, as described previously (2, 38). Peak isometric torque about the axis of the ankle was determined by stimulating the nerve for 200 ms with 0.1-ms square-wave pulses at a

frequency of 300 Hz and voltage increasing from 2 to 8 V until maximum torque was achieved.

Skeletal Muscle Histomorphology and Protein Analyses

NADH-TR histology. Frozen 10- μ m cross sections were cut at the midbelly of the muscle and placed on microscope slides. Slides were thawed at room temperature for 10 min, incubated with NADH-TR staining solution (0.2 M Tris, 1 mg/ml β -nicotinamide adenine dinucleotide, and 1.3 mg/ml nitro blue tetrazolium) in a 37°C water bath for 5 min, dehydrated in graded alcohols, and mounted. Dark stained fibers were counted as NADH-TR positive. All images were processed and analyzed in a blinded manner, with samples being identified as to treatment. Sections were imaged with a Leica DM5500B microscope (Leica Microsystems, Buffalo Grove, IL) at $\times 10$ magnification. Images were stitched by using the automated tile-scan tool to construct an image of the entire cross section of the soleus muscle. Anatomical muscle cross-sectional area (CSA) was measured by tracing the muscle section border in ImageJ (National Institutes of Health, Bethesda, MD). The total numbers of light and dark fibers in each muscle cross section were counted.

Fiber types and cross-sectional areas. Skeletal muscle fiber typing was performed in soleus and gastrocnemius muscles by immunofluorescence staining of myosin heavy chain (MHC)-positive individual fibers as previously described (63). Frozen 10- μ m cross sections were cut and fixed in ice-cold 4% paraformaldehyde-PBS for 5 min. Sections were stained with primary antibodies for MHC I [Developmental Studies Hybridoma Bank (DSHB) no. BA-F8, mouse IgG2b], IIa (DSHB no. SC-71, mouse IgG1), IIb (DSHB no. BF-F3, mouse IgM), and dystrophin (RB-9024; ThermoFisher). After overnight primary antibody incubation, slides were washed with PBS three times for 5 min each. The samples were then incubated for 1 h with a secondary antibody solution containing Alexa Fluor 350 goat anti-mouse IgG2b (A-21140, Life Technologies), Alexa Fluor 488 goat anti-mouse IgG1 (A-21121; Life Technologies), and Alexa Fluor 546 goat anti-mouse IgM (A-21045; Life Technologies). The proportions of type I (blue fluorescence), type IIa (green fluorescence), type IIb (red fluorescence), and type IIx (unstained) fibers were quantified. Dystrophin was visualized with the following secondary Alexa Fluor 647 goat anti-rabbit IgG. Fiber CSA was assessed with ImageJ software on dystrophin-positive stained fibers.

Total and contractile protein content. A subset of TA and gastrocnemius muscles were homogenized in RIPA lysis buffer containing protease inhibitor tablet (Roche Diagnostics) and phosphatase inhibitor II and III cocktails (Sigma Aldrich) with a bullet blender according to the manufacturer's instructions (Midwest Scientific). Homogenates were centrifuged at 664 g for 10 min at 4°C to remove connective tissue, and the supernatant was collected. Protein lysates were assayed in triplicate for total protein content with a Pierce BCA protein assay kit (catalog no. 23225; ThermoFisher), and quantitative gel electrophoresis was performed to determine contractile protein content of each muscle (47). Contractile protein content is defined here as the content of MHC plus actin for each muscle.

Western blots: pRLC. Protein lysates that were used for contractile protein content were used for measuring phosphorylation of myosin regulatory light chain (RLC) (39). Loading buffer was added to protein lysates (50 μ g), heated for 5 min at 95°C, loaded on 4–20% SDS-PAGE gels, and run at 90 V for 90 min. Proteins were transferred to nitrocellulose membranes and probed for RLC (1:1,000, ab48003; Abcam, Cambridge, UK), phosphorylated RLC (pRLC) (1:10,000, ab2480; Abcam), and GAPDH (1:10,000, G8795; Sigma Aldrich) overnight at 4°C. Membranes were washed, incubated with a secondary antibody for 1 h, washed, and then scanned and quantified with the Odyssey Infrared Imaging System (LI-COR Biosciences).

Oxidative damage. Frozen muscles were homogenized with mortar and pestle in liquid nitrogen and resuspended in a solution containing 20% trichloroacetic acid to prevent oxidation (28, 33). Samples were

fractionated into myofibrillar and cytosolic fractions via centrifugation (18). Protein concentration was determined by nanodrop spectrometer. Samples were diluted to a concentration of 1 mg/ml protein in biotin hydrazide coupling buffer and treated with biotin hydrazide as adapted from Grimsrud et al. (28). Duplicate gels were run; one gel was transferred to PVDF membrane for quantification of oxidized proteins, and the second gel was stained with Coomassie blue to quantify total protein as a loading control. After transfer, the PVDF membrane was blocked in PBS-based Odyssey blocking buffer and probed with IR800-conjugated streptavidin. Membranes were imaged on LI-COR, and the entire signal of each lane was quantified. The bands for contractile proteins, MHC and actin, were also quantified individually and identified by myosin:actin standard. Oxidized protein signal was normalized to the protein loading control within each lane.

Statistical Analyses

Data are presented as means \pm SE. Independent *t*-tests were used to determine differences between *skmER α WT* and *skmER α KO* female mice. Significance was set at $P < 0.05$.

RESULTS

Validation and Specificity of *skmER α KO*

To examine the role of ER α specifically in skeletal muscle, female ER $\alpha^{fl/fl}$ mice were crossed with male HSA-cre mice. To confirm knockout of ER α in HSACre-homozygote *lox3ER $\alpha^{fl/fl}$* mice (*skmER α KO*), mRNA expression of ER α was measured and showed little to no expression in five skeletal muscles of female *skmER α KO* mice compared with *skmER α WT* littermates with normal ER α mRNA expression in liver and uterus (Fig. 1A). Protein analyses confirmed lower ER α in skeletal muscles of *skmER α KO* than *skmER α WT* mice (Fig. 1B). The lack of ER α in skeletal muscles did not appear to disturb estrogenic responses in reproductive organs as shown by uter-

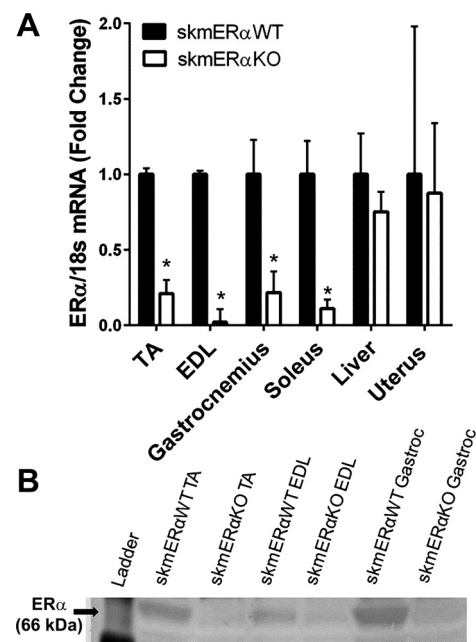


Fig. 1. Verification of knockdown of ER α message and protein specifically in skeletal muscle. A: ER α mRNA expression in female *skmER α WT* and *skmER α KO* mice. B: representative Western blot results showing low ER α protein in muscles of *skmER α KO* mice. The lower ladder band is 50 kDa. *Significantly different from *skmER α WT* ($P \leq 0.017$).

ine mass (76.4 ± 3.2 and 67.7 ± 8.1 mg; $P = 0.383$; Fig. 2A) or estrous cycle of the mice monitored by vaginal cytology (data not shown).

Physical Activity Levels

To determine whether the loss of skeletal muscle ER α was detrimental to the ability and/or motivation for physical movement, multiple measurements of physical activity were made. skmER α WT and skmER α KO female mice did not differ in any of the eight cage activities measured (Table 1). Food consumption was also measured during the same time as the 24-h cage activities and did not differ between skmER α WT and skmER α KO mice (Table 1). An additional form of physical activity, voluntary wheel running, was measured in a separate cohort of female mice, and the distance run by skmER α WT and skmER α KO mice averaged 8 km/24 h for both groups (Table 1).

Body Mass and Composition

Body mass was measured weekly in female mice from weaning until death (Fig. 2B). No differences between skmER α WT and skmER α KO mice were measured until 28 wk of age, when skmER α KO mice became heavier ($P \leq 0.034$; Fig. 2B). By 35 wk of age, female skmER α KO mice weighed 30% more than skmER α WT littermates.

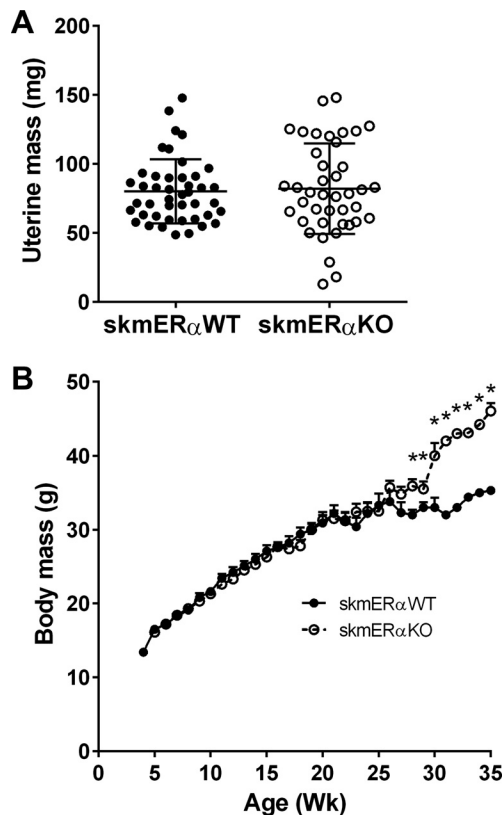


Fig. 2. Phenotypic characteristics of female skmER α WT and skmER α KO mice. A: uterine mass of skmER α WT and skmER α KO mice did not differ ($P = 0.177$). B: weekly body masses of skmER α WT ($n = 19$) and skmER α KO ($n = 16$) female mice from weaning until death at <25 wk of age for physiology experiments were not different. At 28–35 wk of age, skmER α KO mice ($n = 7$) weighed more than skmER α WT mice ($n = 8$). *Significantly different from skmER α WT at corresponding age ($P \leq 0.034$).

Table 1. Physical activities and food intake by female skmER α WT and skmER α KO mice at 22 wk of age

	skmER α WT	skmER α KO	<i>P</i> Value
24-h Cage activities			
<i>n</i>	12	13	
Vertical count	5,823 (745)	6,701 (704)	0.400
Stereotypic count	48,076 (3,406)	49,987 (2,675)	0.660
Jump count	1,219 (185)	1,696 (263)	0.159
Ambulation distance, m/24 h	995 (239)	901 (162)	0.745
Ambulation time, min/24 h	118 (14)	129 (12)	0.538
Stereotypic time, min/24 h	125 (6)	128 (6)	0.682
Jump time, min/24 h	7 (1)	10 (2)	0.163
Total active time, min/24 h	250 (15)	268 (14)	0.375
Food intake, g/24 h	3.4 (0.8)	3.2 (1.1)	0.630
Wheel running			
<i>n</i>	11	10	
Distance during 2nd week, km/24 h	7.97 (0.42)	8.06 (0.38)	0.475

Values are means (SE).

Subcutaneous and visceral fat pad masses did not differ between skmER α WT and skmER α KO mice at 22 or 35 wk of age (Table 2). Similarly, total body lean and fat masses did not differ significantly between skmER α WT and skmER α KO mice at 34 wk of age (Table 2).

Contractility of Isolated Muscles

The size of the soleus muscle (mass, L_0 , CSA) did not differ between female skmER α WT and skmER α KO mice (Table 3). Force production also did not differ (Table 3 and Fig. 3A). Force tracings from twitch and tetanic contractions were analyzed to determine whether contraction kinetics differed between soleus muscles with and without ER α . Neither twitch contraction or relaxation times nor tetanic rates of contraction or relaxation differed between female skmER α WT and skmER α KO mice (Table 3).

We previously showed that estradiol can protect soleus muscle from fatigue (27); therefore, to determine whether estradiol works through ER α to elicit this effect, soleus muscles from a subset of female mice completed a bout of sub-maximal fatiguing contractions. There was greater force loss by skmER α KO than skmER α WT mice from contraction 46 to contraction 60 ($P \leq 0.043$; Fig. 3B). Similarly, maximal isometric force was lower in soleus muscles from skmER α KO than skmER α WT mice immediately after the fatigue contrac-

Table 2. Body and fat pad masses and body composition of female skmER α WT and skmER α KO mice

	skmER α WT	skmER α KO	<i>P</i> Value
22 wk of age			
<i>n</i>	21	20	
Body mass, g	25.8 (0.9)	27.6 (0.8)	0.145
Subcutaneous fat pad mass, g	1.39 (0.1)	1.30 (0.2)	0.687
Visceral fat pad mass, g	1.82 (0.2)	1.56 (0.2)	0.351
34–35 wk of age			
<i>n</i>	6	5	
Body mass, g	31.8 (3.0)	34.1 (2.4)	0.569
Lean mass, g	19.2 (0.7)	19.0 (0.6)	0.835
Fat mass, g	11.8 (2.4)	14.4 (1.8)	0.439
Subcutaneous fat pad mass, g	1.63 (0.5)	1.99 (0.3)	0.559
Visceral fat pad mass, g	2.04 (0.5)	2.69 (0.3)	0.294

Values are means (SE).

Table 3. *In vitro* contractile properties of soleus and extensor digitorum longus muscles of female *skmER α WT* and *skmER α KO* mice at 22 wk of age

	<i>skmERαWT</i>	<i>skmERαKO</i>	<i>P</i> Value
Soleus muscle			
<i>n</i>	15	16	
Mass, mg	9.9 (0.5)	10.9 (0.4)	0.114
Optimal muscle length, mm	8.9 (0.2)	9.3 (0.2)	0.240
Physiological CSA, mm ²	1.47 (0.066)	1.56 (0.051)	0.275
Peak twitch force, mN	20.0 (0.9)	21.6 (1.3)	0.310
Twitch time to peak force, ms	31.2 (0.7)	34.2 (0.8)	0.013
Twitch one-half relaxation time, ms	39.5 (1.7)	37.9 (1.7)	0.563
<i>P</i> ₀ , mN	152.9 (5.0)	157.7 (7.3)	0.599
+dP/dt, N/s	1.7 (0.05)	1.8 (0.09)	0.172
-dP/dt, N/s	2.1 (0.07)	2.3 (0.2)	0.147
Active stiffness, N/m	326.6 (10.9)	324.6 (17.7)	0.926
Peak concentric force, mN	44.1 (2.8)	40.7 (2.9)	0.423
Peak eccentric force, mN	292.0 (12.2)	310.7 (13.1)	0.309
Freq50, Hz	21.4 (0.6)	21.6 (1.0)	0.921
Extensor digitorum longus muscle			
<i>n</i>	13	15	
Mass, mg	9.2 (0.2)	9.1 (0.3)	0.743
Optimal muscle length, mm	10.5 (0.2)	10.7 (0.3)	0.688
Physiological CSA, mm ²	1.87 (0.042)	1.80 (0.058)	0.582
Peak twitch force, mN	87.2 (5.1)	89.5 (5.0)	0.766
Twitch time to peak force, ms	20.4 (1.0)	22.3 (0.4)	0.182
Twitch one-half relaxation time, ms	20.1 (1.2)	24.6 (1.3)	0.034
<i>P</i> ₀ , mN	319.7 (8.9)	296.6 (11.9)	0.091
+dP/dt, N/s	9.0 (0.3)	8.8 (0.4)	0.675
-dP/dt, N/s	15.2 (1.2)	11.2 (1.04)	0.024
Active stiffness, N/m	614.0 (29.7)	610.9 (34.1)	0.947
Peak concentric force, mN	130.7 (8.4)	114.7 (11.1)	0.057
Peak eccentric force, mN	558.2 (19.5)	478.9 (27.8)	0.031
Freq50, Hz	31.7 (2.0)	26.1 (1.3)	0.034

Values are means (SE). CSA, cross-sectional area; *P*₀, maximal isometric tetanic force; +dP/dt, maximum rate of tetanic force development, -dP/dt, maximum rate of tetanic relaxation, Freq50, frequency at which 50% isometric tetanic force is generated.

tions (37.6 ± 3.2 and 23.2 ± 2.7 mN, respectively; $P = 0.032$; Fig. 3C) Soleus muscles from *skmER α KO* mice recovered significantly less force from contraction-induced fatigue compared with *skmER α WT* mice 5, 10, 15, and 20 min after the fatigue protocol ($P \leq 0.039$; Fig. 3C).

Mass, length, and CSA of the EDL muscle did not differ between genotypes (Table 3). Although muscle size was not affected in EDL muscles from *skmER α KO* mice, there were impairments in force generation. Isometric forces at the four highest stimulation frequencies were lower in *skmER α KO* than *skmER α WT* mice (Fig. 4A), and the frequency at which 50% isometric tetanic force is generated (Freq50) was significantly lower in EDL muscles from *skmER α KO* mice (Table 3). EDL muscles from *skmER α KO* mice also produced 16% less eccentric force compared with those from *skmER α WT* mice (Table 3). Peak concentric torque was not significantly different, though it tended to be lower in *skmER α KO* mice (Table 3). Twitch and tetanic contraction kinetics of the EDL muscle did not differ between genotypes, except for -dP/dt, which was slow in muscles from *skmER α KO* mice (Table 3).

A fatiguing protocol of 30 contractions was completed on EDL muscles and induced ~50% force loss that did not differ between *skmER α WT* and *skmER α KO* (Fig. 4B). The recovery of force after the fatiguing protocol also did not differ between groups (Fig. 4C).

Soleus Muscle Composition

To begin to explore whether the greater fatigability and impaired recovery from fatigue were related to alterations in the metabolic profile of the soleus muscle from *skmER α KO* mice, NADH-TR histology was performed (Fig. 5A). The percentage of fibers positive for NADH was 11% greater in soleus muscles from *skmER α KO* compared with *skmER α WT*

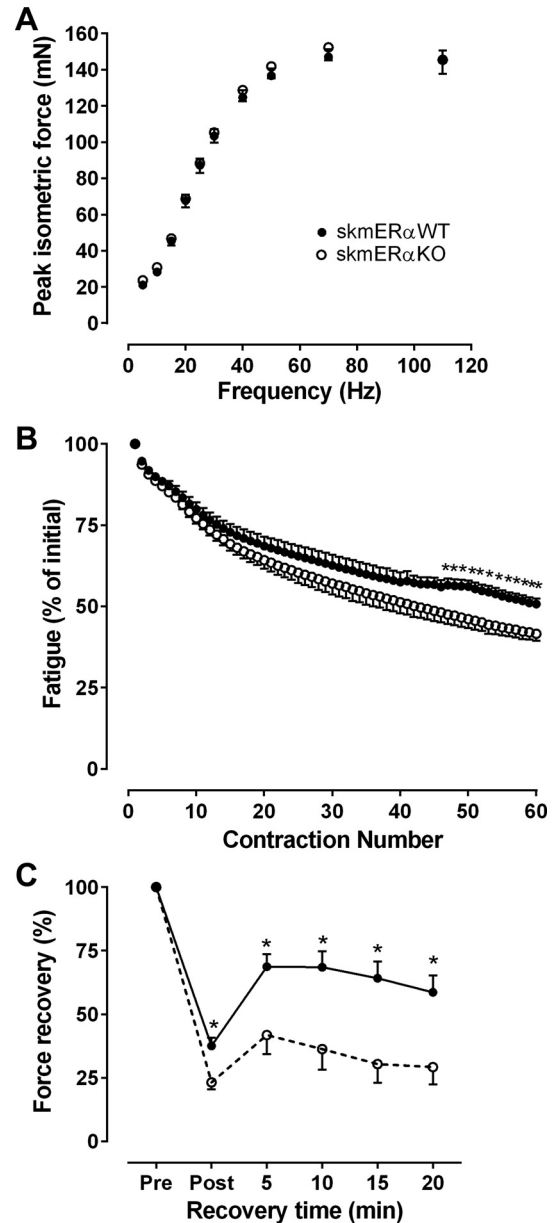


Fig. 3. Contractility of isolated soleus muscles from female *skmER α WT* and *skmER α KO* mice at 22 wk of age. *A*: submaximal and maximal isometric forces did not differ between *skmER α WT* ($n = 15$) and *skmER α KO* ($n = 16$) mice ($P \geq 0.133$). *B*: fatigue is expressed as % of force relative to that of the 1st contraction of the protocol. Beginning at contraction 46, muscles lacking ER α generated less force. *C*: force recovery was calculated as % change from Pre maximal isometric tetanic force (*P*₀). The recovery of soleus muscle *P*₀ was measured after the fatiguing contraction protocol. At every 5-min interval, including Post, which was immediately after the fatiguing contractions, soleus muscles from *skmER α KO* mice ($n = 8$) recovered less *P*₀ than those from *skmER α WT* mice ($n = 7$) ($P \leq 0.043$). *Significantly different from *skmER α WT*.

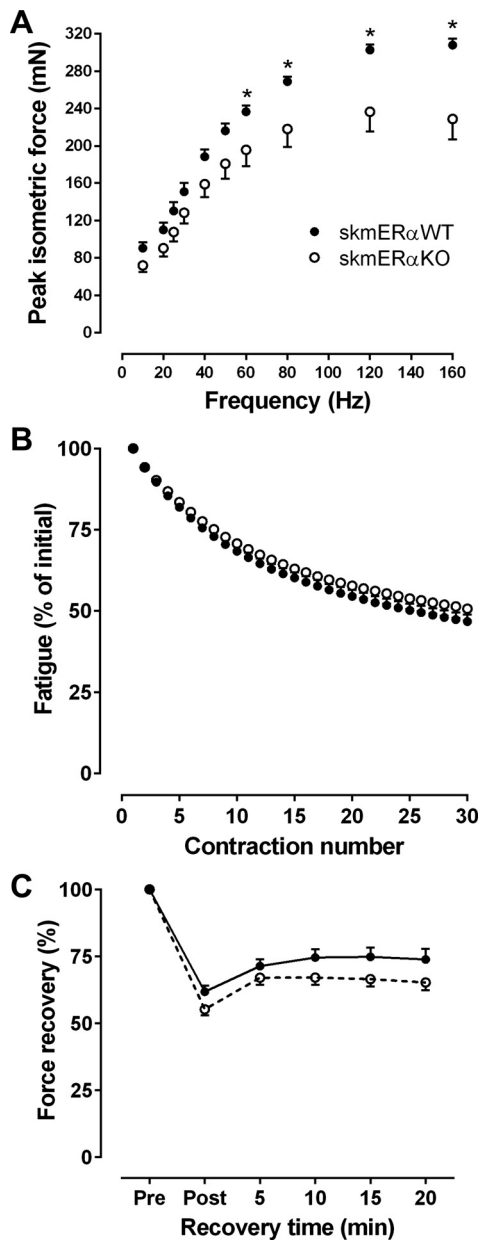


Fig. 4. Contractility of isolated EDL muscles from female skmER α WT and skmER α KO mice at 22 wk of age. *A*: submaximal forces were lower in skmER α KO mice ($n = 15$) compared with skmER α WT mice ($n = 13$) at 60, 80, and 120 Hz stimulation frequencies ($P \leq 0.047$). Maximal force, at 160 Hz, was also lower in skmER α KO compared with skmER α WT mice ($P < 0.001$). *B*: fatigue is expressed as % of force relative to that of the 1st contraction of the protocol. There were no differences between skmER α WT ($n = 5$) and skmER α KO ($n = 6$) mice for any of the 30 fatiguing contractions ($P \geq 0.108$). *C*: EDL muscle recovery of P_0 did not differ between genotypes ($P \geq 0.070$). *Significantly different from skmER α WT.

mice ($P = 0.015$; Fig. 5C). Soleus muscle anatomical CSA and fiber number did not differ between genotypes ($P \geq 0.669$; Fig. 5B).

Soleus muscle fiber type distribution and fiber CSA were also measured (Fig. 5, D–F). There were no statistical differences in type II fiber composition of soleus muscle between skmER α WT and skmER α KO mice ($P \geq 0.147$), although there was a trend for fewer type I fibers in skmER α KO mice

($P = 0.055$). Soleus fiber CSAs did not differ for any fiber type between skmER α KO and skmER α WT mice ($P > 0.132$). While size of soleus muscles (physiological and anatomical CSAs and length) and size of fibers (CSA and number) did not significantly differ between skmER α WT and skmER α KO mice, all variables trended toward being bigger in the skmER α KO mice, including muscle mass (Table 3).

In Vivo Skeletal Muscle Contractility

To further analyze contractility of muscle groups critical for ambulation, *in vivo* maximal and submaximal muscle strength and power of the plantarflexors were measured. Peak isometric torque was 16% less in skmER α KO compared with skmER α WT littermates ($P = 0.001$; Fig. 6A). skmER α KO mice also produced lower maximal concentric torque than skmER α WT mice ($P < 0.001$), and maximal eccentric torque was not significantly different, though it tended to be lower in skmER α KO mice ($P = 0.084$; Fig. 6A). Moreover, when the plantarflexor muscles were stimulated at submaximal frequencies, skmER α KO mice produced less submaximal torque at every frequency compared with skmER α WT mice ($P < 0.05$; Fig. 6B). skmER α KO mice also require a greater stimulation frequency to generate 50% of maximal isometric torque than skmER α WT mice ($P = 0.042$; Fig. 6C). skmER α KO mice produced less concentric torque from 0 to 1,200°/s (Fig. 6D), generated 20–30% less power across all velocities tested (Fig. 6E), and generated less peak isometric torque at nine ankle angles (Fig. 6F) compared with skmER α WT mice. Maximal rates of torque development and relaxation ($+dP/dt$ and $-dP/dt$) of the plantarflexors did not differ between skmER α WT and skmER α KO mice ($P \geq 0.240$).

In a separate group of mice, peak isometric torque of the dorsiflexors was measured. Consistent with the plantarflexors, the dorsiflexors produced 12% less torque in the skmER α KO compared with the skmER α WT female mice ($P < 0.047$; Fig. 7). Size of the major dorsiflexor muscle, the TA, could not explain the low torque in skmER α KO mice, as TA muscle masses did not differ from skmER α WT mice (38.8 ± 0.7 and 39.9 ± 0.8 mg, respectively; $P = 0.604$).

Gastrocnemius Muscle Composition

Gastrocnemius muscle mass also did not differ between skmER α WT and skmER α KO mice (129.7 ± 2.6 and 126.7 ± 2.6 mg, respectively; $P = 0.786$). To further probe whether the low torque and power of the skmER α KO plantarflexors were related to alterations in fiber type or size or contractile protein modifications, additional analyses were conducted on gastrocnemius muscles. There were no differences in fiber type composition of the gastrocnemius muscle between skmER α KO and skmER α WT mice ($P > 0.100$; Fig. 8A). Type I and type IIb fibers from gastrocnemius muscle of skmER α KO mice had 21% and 14% smaller CSAs, respectively, compared with those from skmER α WT mice ($P \leq 0.047$; Fig. 8B). Total protein and contractile protein contents were measured in gastrocnemius muscles, but no differences were observed between those from skmER α KO and skmER α WT mice ($P = 0.960$ and $P = 0.429$, respectively; Fig. 8C).

To determine whether there were qualitative differences in contractile proteins between skmER α WT and skmER α KO

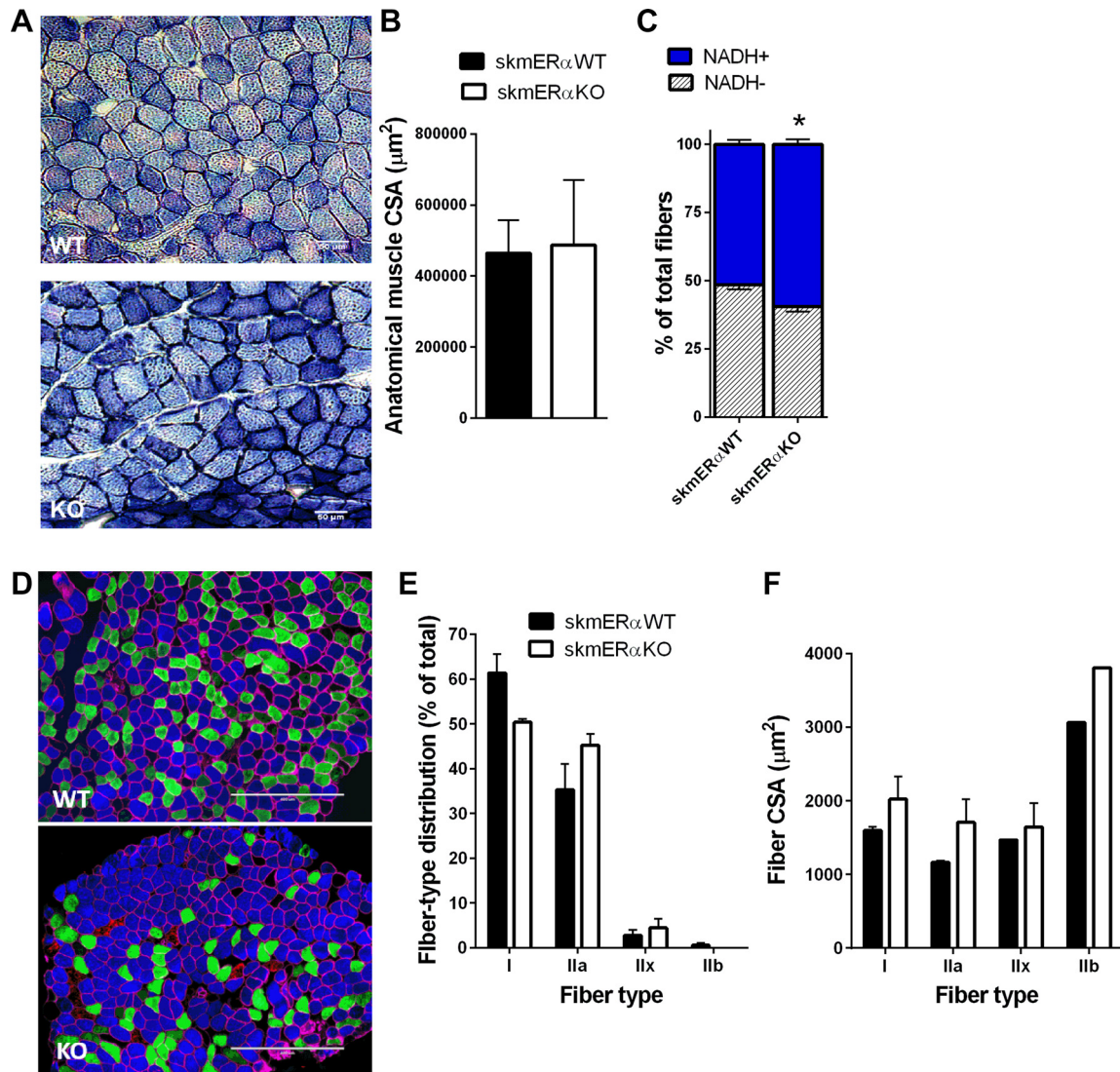


Fig. 5. Factors that could influence fatigability of soleus muscle. *A*: representative images of NADH-TR staining of soleus muscle cross sections from female skmER α WT and skmER α KO mice. Dark blue, NADH⁺ fibers; light blue, NADH⁻ fibers. *B*: anatomical muscle cross-sectional area (CSA) did not differ between skmER α WT ($n = 5$) and skmER α KO ($n = 4$) mice ($P > 0.834$). *C*: % of NADH⁺ fibers was greater in skmER α KO than skmER α WT mice ($P = 0.015$). *D*: representative images of skeletal muscle fiber typing in cross sections of soleus muscles from skmER α WT and skmER α KO mice. Myosin heavy chain isoform staining is as follows: type I (blue), type IIa (green), type IIb (red), and type IIX (unstained) fibers. Muscle fiber border depicted by dystrophin (pink). *E*: fiber type distribution in soleus muscles from skmER α WT ($n = 5$) and skmER α KO ($n = 4$) mice did not differ ($P > 0.055$). *F*: CSA by fiber type in skmER α WT and skmER α KO soleus muscles did not differ ($P > 0.132$). *Significantly different from skmER α WT.

muscles, oxidative damage to gastrocnemius muscle proteins was measured by biotin hydrazide tagging. Oxidative damage to proteins in the myofibrillar and cytosolic fractions did not differ between skmER α KO and skmER α WT mice ($P \geq 0.504$), nor were there differences in oxidative damage specifically to MHC or actin between muscle with and without ER α ($P \geq 0.316$).

Consistent with total and contractile protein contents, the content of myosin RLC in gastrocnemius and TA muscles did not differ between skmER α WT and skmER α KO mice ($P \geq 0.075$; Fig. 8*D*). However, phosphorylation of the RLC was lower by ~90% in muscles from skmER α KO compared with skmER α WT mice ($P \leq 0.047$; Fig. 8, *D* and *E*).

DISCUSSION

Estradiol impacts skeletal muscle contractility, and here we tested the hypothesis that ER α is a primary ER in muscle fibers

that estradiol utilizes to elicit its beneficial effects on contractile functions. Our data support the hypothesis that ER α is critical for optimal muscle contractility by demonstrating that mice lacking ER α specifically in skeletal muscle fibers are weaker. We base this conclusion on comprehensive contractility measurements of two muscles assessed *in vitro* and two major muscle groups assessed *in vivo* with maximal and submaximal isometric and dynamic contractions and analyzing force-related outcomes such as power and recovery of force after fatigue. Collectively our results are in agreement with the work by Ribas and coworkers demonstrating that ER α is necessary for overall skeletal muscle health (59).

The major finding of this study was that the ability of skeletal muscle to generate force was impaired, as systematically shown in plantarflexor and dorsiflexor muscle groups as well as isolated soleus and EDL muscles in female

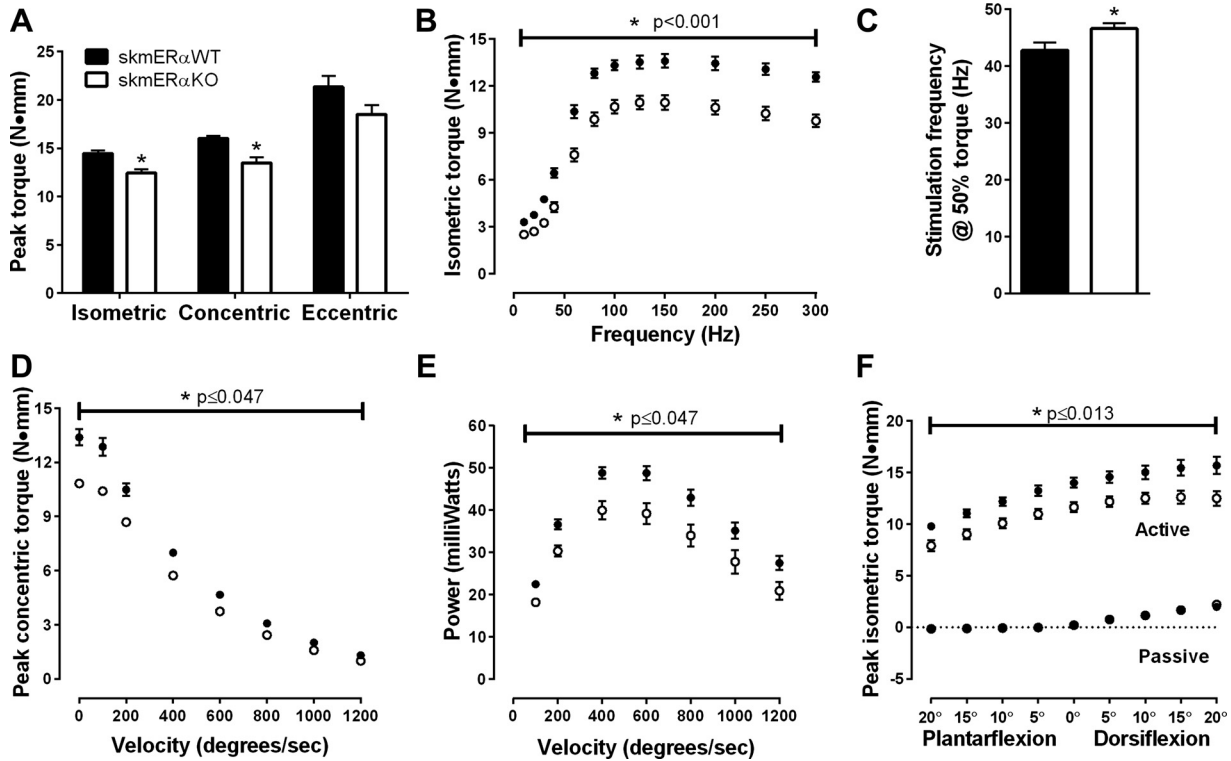


Fig. 6. In vivo plantarflexor muscle contractility in female skmER α WT and skmER α KO mice at 22 wk of age. *A*: peak isometric and peak concentric torques were lower in skmER α KO mice ($n = 9$) compared with skmER α WT mice ($n = 9$) ($P = 0.001$). Peak eccentric torque did not differ between groups ($P = 0.080$). *B*: submaximal and maximal torques were lower in skmER α KO mice compared with skmER α WT mice at each stimulation frequency ($P < 0.001$). *C*: frequency at which plantarflexor muscles produced 50% torque was greater in skmER α KO mice than in skmER α WT mice ($P < 0.001$). *D*: skmER α KO mice produced less concentric torque at all velocities between 0 (isometric) and 1,200°/s compared with skmER α WT mice ($P \leq 0.047$). *E*: power produced at each velocity was lower in skmER α KO mice than skmER α WT mice ($P \leq 0.047$). *F*: active torque at different ankle angles was lower in skmER α KO mice compared with skmER α WT mice ($P \leq 0.013$). Passive torque did not differ between the groups ($P \geq 0.264$). *Significantly different from skmER α WT.

skmER α KO mice. As expected with the diversity of functions that these hindlimb muscles perform in vivo, the force impairments manifested differently across muscles and muscle groups. The plantarflexors in these mice were particularly affected, having low submaximal and maximal isometric torques, low peak concentric torque across a range of velocities and at multiple ankle angles, and reduced power compared

with skmER α WT littermates (Fig. 6). These are physiologically relevant measurements of contractility, meaningful beyond those restricted to maximal isometric contractions, and furthermore were made in vivo, permitting analyses of a muscle's contractile function in its natural environment. Peak isometric torque of the dorsiflexors was similarly low (Fig. 7), as were submaximal (Fig. 4A) and peak eccentric tetanic forces of isolated EDL muscles from skmER α KO mice (Table 3). Collectively, these results demonstrate that deficiency of ER α in skeletal muscle fibers detrimentally impacts force generation, consistent with a previous report that isometric force was affected in some skeletal muscles of whole body ER α -knockout mice (10). Beyond hindlimb skeletal muscle, ER α has been implicated as a key ER in rodent cardiac (52, 53, 55, 71) and genioglossal (34, 40) muscle contractile function.

The force impairment in skmER α KO mice manifested differently in soleus muscles. Maximal and submaximal force generation was not affected in soleus muscles from female skmER α KO mice, but the ability to sustain force during repetitive contractions, that is, during a fatigue protocol, was impaired (Fig. 3B). This result is consistent with a previous report indicating that soleus muscle lacking ER α had low fatigue resistance (59). Our data expand on that result by linking ER α not only with muscle fatigability but also with the recovery from fatigue. Soleus muscle lacking ER α did not recover the ability to generate force after a series of repetitive fatiguing contractions to the same extent as soleus muscle

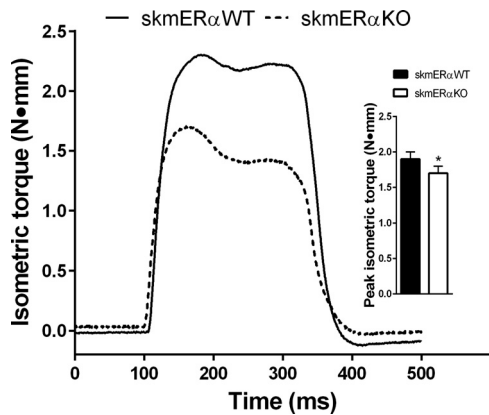


Fig. 7. Peak isometric in vivo dorsiflexor muscle torque in female skmER α WT and skmER α KO mice at 22 wk of age: representative isometric tetanic torque tracings of dorsiflexor muscles from skmER α WT and skmER α KO mice measured in vivo. *Inset*: peak isometric torque was lower in female skmER α KO ($n = 19$) than skmER α WT ($n = 20$) mice. *Significantly different from skmER α WT ($P = 0.047$).

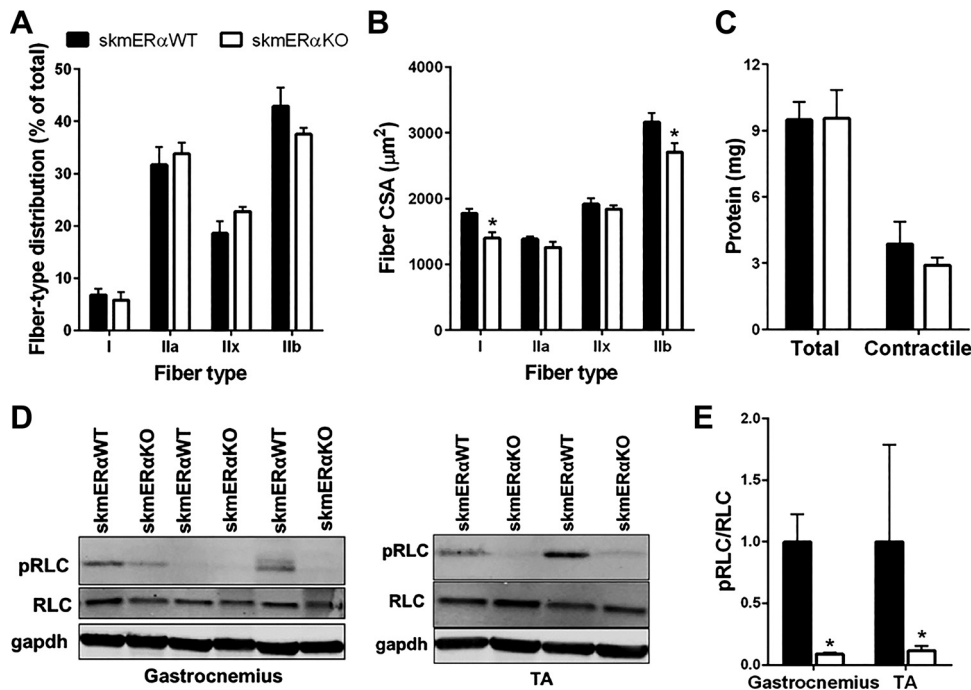


Fig. 8. Factors that could influence muscle contractility of the gastrocnemius and tibialis anterior (TA) muscles. *A*: fiber type distribution in gastrocnemius muscles from female skmER α WT ($n = 4$) and skmER α KO ($n = 4$) mice did not differ ($P \geq 0.100$). *B*: cross-sectional area (CSA) by fiber type from skmER α WT and skmER α KO mice showed that type I and type I Ib fibers are smaller in gastrocnemius muscles of skmER α KO mice compared with those of skmER α WT mice. *C*: total and contractile protein content did not differ between skmER α WT ($n = 4$) and skmER α KO ($n = 4$) mice ($P \geq 0.429$). *D*: representative Western blots of phosphorylated myosin regulatory light chain (pRLC), myosin regulatory light chain (RLC), and GAPDH as loading control in gastrocnemius and TA muscles from skmER α WT and skmER α KO mice. *E*: pRLC relative to total RLC is lower in gastrocnemius and TA muscles of skmER α KO ($n = 4$) mice compared with skmER α WT ($n = 4$) mice ($P \leq 0.047$). *Significantly different from skmER α WT.

containing ER α (Fig. 3C), even though soleus muscles from skmER α KO had a greater percentage of oxidative muscle fibers as indicated by those positive for NADH (Fig. 5C). Such outcomes may be related to ER α 's role in muscle metabolism that may include optimal mitochondrial function (59, 60), although recent evidence shows that localization of estradiol to mitochondria in skeletal muscle is independent of ER α (66). Thus, directed experiments specifically designed to address connections between estradiol, ERs, fatigue, and mitochondrial function (e.g., ATP production) in skeletal muscle fibers are warranted.

Skeletal muscle contractility can be affected by physical (in)activity, and estradiol status is a strong regulator of physical (in)activity in female rodents (see, e.g., Refs. 8, 41). Therefore, it was important to measure possible effects of manipulation of skeletal muscle ER α on physical activity of the mice. We comprehensively show that physical activities in the cage and voluntary wheel running are unaffected by the elimination of ER α in skeletal muscle (Table 1). These results provide evidence that the changes we measured in skeletal muscle contractility, such as force and power, are not due to physical inactivity and consequential muscle disuse in the skmER α KO mice and instead can be directly attributed to lack of ER α in skeletal muscle fibers and presumably diminished estradiol signaling. Given reports that mice lacking skeletal muscle ER α have impaired mitochondria (59), it is interesting that capacity for physical activity in terms of cage movement and voluntary wheel running was not reduced in skmER α KO mice, suggesting that mice would need to engage in intense exercise to possibly see performance deficits.

In addition to physical activities of female mice not being affected by the lack of ER α , food intake (Table 1), body mass (Fig. 2B), and subcutaneous and visceral fat pad masses (Table 2) did not differ between skmER α KO and skmER α WT female mice at 22 wk of age. However, at ~26 wk of age body mass of skmER α WT mice plateaued while that of skmER α KO mice

continued to increase, and by 34 wk of age skmER α KO mice weighed 30% more (Fig. 2B). A similar delayed increase in body mass has been reported in whole body ER α -knockout female mice (42, 68) and in skeletal muscle ER α -knockout female mice (59). To determine whether the larger body mass of the ER α KO mice was due to preferential gain of lean or fat mass, echoMRI was performed on 34-wk-old mice. No differences in lean or fat mass were measured between skmER α WT and skmER α KO mice (Table 2). This result differs from that in whole body ER α -knockout female mice, in which the percentage of body mass comprised of fat was high (42). Because the distribution of lean and fat mass as well as overall metabolic health can influence muscle contractility, it will be important for future studies to evaluate how chronic deficiency of skeletal muscle ER α , that is, aging, of these mice affects muscle force generation.

Considering factors that contribute to low skeletal muscle force generation, the most direct is muscle size; however, wet masses of hindlimb skeletal muscles measured for contractility did not differ between skmER α KO and skmER α WT female mice. We further assessed the gastrocnemius muscle because it is the major muscle comprising the plantarflexors, which showed impaired torque and power in the skmER α KO mice. In addition to wet mass of this muscle not differing between skmER α KO and skmER α WT female mice, total protein, contractile proteins (MHC and actin), and total RLC content also did not differ (Fig. 8, C and D). Fiber type distribution based on MHC isoforms did not differ between gastrocnemius muscles of skmER α KO and skmER α WT female mice (Fig. 8A). Thus, the amount of contractile proteins and myosin isoform composition do not help to explain contractility impairments in the skmER α KO mice such as power. This is consistent with another report demonstrating that estradiol mediates effects on MHC isoform expression in skeletal muscle through ER β rather than ER α (67). CSAs of MHC I Ia and MHC I Ix fibers also did not differ between gastrocnemius muscles from

skmER α KO and skmER α WT female mice, although MHC I and MHC IIb fibers had smaller CSAs in those from skmER α KO than skmER α WT mice (Fig. 8B). Because MHC I and IIb fibers together comprise about one-half of the fibers in mouse gastrocnemius muscle, this may explain a portion of the reduced force generating capacity of skmER α KO plantarflexors but is not plausible to explain the impairment in full.

The capacity of myosin to bind strongly to actin and generate force in skeletal muscle of female mice (25, 46, 47) and women (58) is impaired with estradiol deficiency. Posttranslational modification of contractile proteins, particularly MHC, can affect force generation (58), although in the present study oxidative damage to myosin or actin was not detected. Phosphorylation of contractile proteins such as the RLC of myosin is another posttranslational modification that is known to affect force production. Because RLC phosphorylation is reduced in skeletal muscle of ovariectomized mice (39) and in fibers of aged women (44) and is lowered by ER inhibitors in C2C12 cells (39), we focused on this contractile protein modification to potentially explain reduced force generation in gastrocnemius and TA muscles. Consistent with those previous reports, we measured a substantial reduction in phosphorylation of the myosin RLC in muscles of skmER α KO mice, indicating that estradiol utilizes ER α to phosphorylate RLC, which in turn allows for a greater capacity of myosin to bind strongly to actin and generate force. Previously it was suggested that estradiol mediates RLC phosphorylation through ER β and GPER, but those experiments were conducted on C2C12 cells (39). Results here support the hypothesis that in muscle fibers ER α is a mode through which estradiol affects pRLC and skeletal muscle contractility. Furthermore, the magnitude of force deficits we have previously measured in muscles of estradiol-deficient female mice has been 10–20% (25, 46, 47, 69) and is similar to the magnitude of force, torque, and power deficits measured in muscles with an ER α deficiency.

Early evidence that estradiol mediates its effects in skeletal muscle through ERs came from Dieli-Conwright and coworkers (17). Results presented here show that ER α is a specific receptor necessary for optimal contractile function in female muscle, further substantiating that mechanisms underlying estradiol's beneficial impact on skeletal muscle are important to elucidate in order to understand relationships between hormone deficiency and sarcopenia. The maintenance of strength across the life span and with the loss of ovarian function is critical for women to maintain functional independence. This point is further emphasized by the fact that women live nearly one-third of their lives after menopause. Because of the controversial results of the Women's Health Initiative, standard approaches for pharmacological activation of ER α are not employed with the same frequency as they were before that initiative; however, our data strongly suggest that ER α is critical for normal physiological function of skeletal. Thus, identification of novel compounds that could activate ER α might provide alternative therapeutic interventions to help women maintain strength and independence throughout their life span.

ACKNOWLEDGMENTS

We thank Nardina Nash for assistance with breeding mice, Vineesha Kollipara, Sira Karvinen, Serena Mooney, and Ananya Koripella for technical

assistance, Dave Thomas for purified rabbit myosin, and Ken Korach/Andrea Hevener and James Ervasti for ER α floxed mice and HSA-cre mice, respectively.

GRANTS

Our research has been supported by National Institutes of Health Grants R01 AG-031743 (D. A. Lowe), T32 AR-007612 (B. C. Collins and C. A. Cabelka), and T32 AG-0299796 (T. L. Mader); a grant from the Office of the Vice President for Research, University of Minnesota (D. A. Lowe); and a grant from the American Diabetes Association (BS-1-15-170, E. E. Spangenburg). T. L. Mader and B. C. Collins were also supported by a University of Minnesota Doctoral Dissertation Fellowship and Interdisciplinary Doctoral Fellowship, respectively.

DISCLOSURES

No conflicts of interest, financial or otherwise, are declared by the authors.

AUTHOR CONTRIBUTIONS

B.C.C., E.E.S., and D.A.L. conceived and designed research; B.C.C., T.L.M., C.A.C., M.R.I., E.E.S., and D.A.L. performed experiments; B.C.C., T.L.M., C.A.C., M.R.I., E.E.S., and D.A.L. analyzed data; B.C.C., T.L.M., C.A.C., M.R.I., E.E.S., and D.A.L. interpreted results of experiments; B.C.C. and E.E.S. prepared figures; B.C.C. and D.A.L. drafted manuscript; B.C.C., T.L.M., C.A.C., E.E.S., and D.A.L. edited and revised manuscript; B.C.C., T.L.M., C.A.C., M.R.I., E.E.S., and D.A.L. approved final version of manuscript.

REFERENCES

- Baltgalvis KA, Call JA, Cochrane GD, Laker RC, Yan Z, Lowe DA. Exercise training improves plantar flexor muscle function in mdx mice. *Med Sci Sports Exerc* 44: 1671–1679, 2012. doi:10.1249/MSS.0b013e31825703f0.
- Baltgalvis KA, Call JA, Nikas JB, Lowe DA. Effects of prednisolone on skeletal muscle contractility in mdx mice. *Muscle Nerve* 40: 443–454, 2009. doi:10.1002/mus.21327.
- Baltgalvis KA, Jaeger MA, Fitzsimons DP, Thayer SA, Lowe DA, Ervasti JM. Transgenic overexpression of γ -cytoplasmic actin protects against eccentric contraction-induced force loss in mdx mice. *Skeletal Muscle* 1: 32, 2011. doi:10.1186/2044-5040-1-32.
- Barros RP, Gabbi C, Morani A, Warner M, Gustafsson JA. Participation of ERalpha and ERbeta in glucose homeostasis in skeletal muscle and white adipose tissue. *Am J Physiol Endocrinol Metab* 297: E124–E133, 2009. doi:10.1152/ajpendo.00189.2009.
- Barros RP, Machado UF, Warner M, Gustafsson JA. Muscle GLUT4 regulation by estrogen receptors ERbeta and ERalpha. *Proc Natl Acad Sci USA* 103: 1605–1608, 2006 (Erratum. *Proc Natl Acad Sci USA* 103: 8298–8299, 2006). doi:10.1073/pnas.0510391103.
- Bonen A, Clark MG, Henriksen EJ. Experimental approaches in muscle metabolism: hindlimb perfusion and isolated muscle incubations. *Am J Physiol Endocrinol Metab* 266: E1–E16, 1994. doi:10.1152/ajpendo.1994.266.1.E1.
- Bouchard DR, Héroux M, Janssen I. Association between muscle mass, leg strength, and fat mass with physical function in older adults: influence of age and sex. *J Aging Health* 23: 313–328, 2011. doi:10.1177/0898264310388562.
- Bowen RS, Turner MJ, Lightfoot JT. Sex hormone effects on physical activity levels: why doesn't Jane run as much as Dick? *Sports Med* 41: 73–86, 2011. doi:10.2165/11536860-000000000-00000.
- Brady AO, Straight CR, Evans EM. Body composition, muscle capacity, and physical function in older adults: an integrated conceptual model. *J Aging Phys Act* 22: 441–452, 2014. doi:10.1123/JAPA.2013-0009.
- Brown M, Ning J, Ferreira JA, Bogener JL, Lubahn DB. Estrogen receptor-alpha and -beta and aromatase knockout effects on lower limb muscle mass and contractile function in female mice. *Am J Physiol Endocrinol Metab* 296: E854–E861, 2009. doi:10.1152/ajpendo.90696.2008.
- Bryzgalova G, Gao H, Ahren B, Zierath JR, Galuska D, Steiler TL, Dahlman-Wright K, Nilsson S, Gustafsson JA, Efendic S, Khan A. Evidence that oestrogen receptor-alpha plays an important role in the regulation of glucose homeostasis in mice: insulin sensitivity in the liver. *Diabetologia* 49: 588–597, 2006. doi:10.1007/s00125-005-0105-3.

12. Call JA, Eckhoff MD, Baltgalvis KA, Warren GL, Lowe DA. Adaptive strength gains in dystrophic muscle exposed to repeated bouts of eccentric contraction. *J Appl Physiol* (1985) 111: 1768–1777, 2011. doi:10.1152/jappphysiol.00942.2011.
13. Capllonch-Amer G, Sbert-Roig M, Galmés-Pascual BM, Proenza AM, Lladó I, Gianotti M, García-Palmer FJ. Estradiol stimulates mitochondrial biogenesis and adiponectin expression in skeletal muscle. *J Endocrinol* 221: 391–403, 2014. doi:10.1530/JOE-14-0008.
14. Cawthon PM, Fox KM, Gandra SR, Delmonico MJ, Chiou CF, Anthony MS, Sewall A, Goodpaster B, Satterfield S, Cummings SR, Harris TB; Health, Aging and Body Composition Study. Do muscle mass, muscle density, strength, and physical function similarly influence risk of hospitalization in older adults? *J Am Geriatr Soc* 57: 1411–1419, 2009. doi:10.1111/j.1532-5415.2009.02366.x.
15. Cheskis BJ, Greger JG, Nagpal S, Freedman LP. Signaling by estrogens. *J Cell Physiol* 213: 610–617, 2007. doi:10.1002/jcp.21253.
16. Colson BA, Petersen KJ, Collins BC, Lowe DA, Thomas DD. The myosin super-relaxed state is disrupted by estradiol deficiency. *Biochem Biophys Res Commun* 456: 151–155, 2015. doi:10.1016/j.bbrc.2014.11.050.
17. Dieli-Conwright CM, Spektor TM, Rice JC, Todd Schroeder E. Oestradiol and SERM treatments influence oestrogen receptor coregulator gene expression in human skeletal muscle cells. *Acta Physiol (Oxf)* 197: 187–196, 2009. doi:10.1111/j.1748-1716.2009.01997.x.
18. Dimauro I, Pearson T, Caporossi D, Jackson MJ. A simple protocol for the subcellular fractionation of skeletal muscle cells and tissue. *BMC Res Notes* 5: 513, 2012. doi:10.1186/1756-0500-5-513.
19. Dupont S, Krust A, Gansmuller A, Dierich A, Chambon P, Mark M. Effect of single and compound knockouts of estrogen receptors alpha (ERalpha) and beta (ERbeta) on mouse reproductive phenotypes. *Development* 127: 4277–4291, 2000.
20. Finni T, Noorkoiv M, Pöllänen E, Ronkainen PH, Alén M, Kaprio J, Kovanen V, Sipilä S. Muscle function in monozygotic female twin pairs discordant for hormone replacement therapy. *Muscle Nerve* 44: 769–775, 2011. doi:10.1002/mus.22162.
21. Fu MH, Maher AC, Hamadeh MJ, Ye C, Tarnopolsky MA. Exercise, sex, menstrual cycle phase, and 17beta-estradiol influence metabolism-related genes in human skeletal muscle. *Physiol Genomics* 40: 34–47, 2009. doi:10.1152/physiolgenomics.00115.2009.
22. Gómez-Cabello A, Carnicero JA, Alonso-Bouzon C, Tresguerres JA, Alfaro-Acha A, Ara I, Rodríguez-Mañas L, García-García FJ. Age and gender, two key factors in the associations between physical activity and strength during the ageing process. *Maturitas* 78: 106–112, 2014. doi:10.1016/j.maturitas.2014.03.007.
23. Goodpaster BH, Park SW, Harris TB, Kritchevsky SB, Nevitt M, Schwartz AV, Simonsick EM, Tylavsky FA, Visser M, Newman AB. The loss of skeletal muscle strength, mass, and quality in older adults: the health, aging and body composition study. *J Gerontol A Biol Sci Med Sci* 61: 1059–1064, 2006. doi:10.1093/gerona/61.10.1059.
24. Gorres BK, Bomhoff GL, Morris JK, Geiger PC. In vivo stimulation of oestrogen receptor α increases insulin-stimulated skeletal muscle glucose uptake. *J Physiol* 589: 2041–2054, 2011. doi:10.1113/jphysiol.2010.199018.
25. Greising SM, Baltgalvis KA, Kosir AM, Moran AL, Warren GL, Lowe DA. Estradiol's beneficial effect on murine muscle function is independent of muscle activity. *J Appl Physiol* (1985) 110: 109–115, 2011. doi:10.1152/jappphysiol.00852.2010.
26. Greising SM, Baltgalvis KA, Lowe DA, Warren GL. Hormone therapy and skeletal muscle strength: a meta-analysis. *J Gerontol A Biol Sci Med Sci* 64: 1071–1081, 2009. doi:10.1093/gerona/64.10.1071.
27. Greising SM, Carey RS, Blackford JE, Dalton LE, Kosir AM, Lowe DA. Estradiol treatment, physical activity, and muscle function in ovarian-senescent mice. *Exp Gerontol* 46: 685–693, 2011. doi:10.1016/j.exger.2011.04.006.
28. Grimsrud PA, Picklo MJ Sr, Griffin TJ, Bernlohr DA. Carbonylation of adipose proteins in obesity and insulin resistance: identification of adipocyte fatty acid-binding protein as a cellular target of 4-hydroxynonenal. *Mol Cell Proteomics* 6: 624–637, 2007. doi:10.1074/mcp.M600120-MCP200.
29. Heine PA, Taylor JA, Iwamoto GA, Lubahn DB, Cooke PS. Increased adipose tissue in male and female estrogen receptor-alpha knockout mice. *Proc Natl Acad Sci USA* 97: 12729–12734, 2000. doi:10.1073/pnas.97.23.12729.
30. Hevener AL, Clegg DJ, Mauvais-Jarvis F. Impaired estrogen receptor action in the pathogenesis of the metabolic syndrome. *Mol Cell Endocrinol* 418: 306–321, 2015. doi:10.1016/j.mce.2015.05.020.
31. Hewitt SC, Kissling GE, Fieselman KE, Jayes FL, Gerrish KE, Korach KS. Biological and biochemical consequences of global deletion of exon 3 from the ER alpha gene. *FASEB J* 24: 4660–4667, 2010. doi:10.1096/fj.10-163428.
32. Høeg LD, Sjøberg KA, Jeppesen J, Jensen TE, Frøsig C, Birk JB, Bisiani B, Hiscock N, Pilegaard H, Wojtaszewski JF, Richter EA, Kiens B. Lipid-induced insulin resistance affects women less than men and is not accompanied by inflammation or impaired proximal insulin signaling. *Diabetes* 60: 64–73, 2011. doi:10.2337/db10-0698.
33. Horn AF, Barouh N, Nielsen NS, Baron CP, Jacobsen C. Homogenization pressure and temperature affect protein partitioning and oxidative stability of emulsions. *J Am Oil Chem Soc* 90: 1541–1550, 2013. doi:10.1007/s11746-013-2292-2.
34. Hou YX, Jia SS, Liu YH. 17Beta-estradiol accentuates contractility of rat genioglossal muscle via regulation of estrogen receptor alpha. *Arch Oral Biol* 55: 309–317, 2010. doi:10.1016/j.archoralbio.2010.02.002.
35. Hubal MJ, Ingalls CP, Allen MR, Wenke JC, Hogan HA, Bloomfield SA. Effects of eccentric exercise training on cortical bone and muscle strength in the estrogen-deficient mouse. *J Appl Physiol* (1985) 98: 1674–1681, 2005. doi:10.1152/jappphysiol.00275.2004.
36. Katzenellenbogen BS. Estrogen receptors: bioactivities and interactions with cell signaling pathways. *Biol Reprod* 54: 287–293, 1996. doi:10.1095/biolreprod54.2.287.
37. Kim S, Jin Y, Park Y. Estrogen and n-3 polyunsaturated fatty acid supplementation have a synergistic hypotriglyceridemic effect in ovariectomized rats. *Genes Nutr* 10: 475, 2015. doi:10.1007/s12263-015-0475-1.
38. Kosir AM, Mader TL, Greising AG, Novotny SA, Baltgalvis KA, Lowe DA. Influence of ovarian hormones on strength loss in healthy and dystrophic female mice. *Med Sci Sports Exerc* 47: 1177–1187, 2015. doi:10.1249/MSS.0000000000000531.
39. Lai S, Collins BC, Colson BA, Kararigas G, Lowe DA. Estradiol modulates myosin regulatory light chain phosphorylation and contractility in skeletal muscle of female mice. *Am J Physiol Endocrinol Metab* 310: E724–E733, 2016. doi:10.1152/ajpendo.00439.2015.
40. Li W, Liu YH. Effects of phytoestrogen genistein on genioglossus function and oestrogen receptors expression in ovariectomized rats. *Arch Oral Biol* 54: 1029–1034, 2009. doi:10.1016/j.archoralbio.2009.09.002.
41. Lightfoot JT. Sex hormones' regulation of rodent physical activity: a review. *Int J Biol Sci* 4: 126–132, 2008. doi:10.7150/ijbs.4.126.
42. Manrique C, Lastra G, Habibi J, Mugerfeld I, Garro M, Sowers JR. Loss of estrogen receptor α signaling leads to insulin resistance and obesity in young and adult female mice. *Cardiorenal Med* 2: 200–210, 2012. doi:10.1159/000339563.
43. Matic M, Bryzgalova G, Gao H, Antonson P, Humire P, Omoto Y, Portwood N, Pramfalk C, Efendic S, Berggren PO, Gustafsson JA, Dahlman-Wright K. Estrogen signalling and the metabolic syndrome: targeting the hepatic estrogen receptor alpha action. *PLoS One* 8: e57458, 2013. doi:10.1371/journal.pone.0057458.
44. Miller MS, Bedrin NG, Callahan DM, Previs MJ, Jennings ME 2nd, Ades PA, Maughan DW, Palmer BM, Toth MJ. Age-related slowing of myosin actin cross-bridge kinetics is sex specific and predicts decrements in whole skeletal muscle performance in humans. *J Appl Physiol* (1985) 115: 1004–1014, 2013. doi:10.1152/jappphysiol.00563.2013.
45. Miniou P, Tiziano D, Frugier T, Roblot N, Le Meur M, Melki J. Gene targeting restricted to mouse striated muscle lineage. *Nucleic Acids Res* 27: e27, 1999. doi:10.1093/nar/27.19.e27.
46. Moran AL, Nelson SA, Landisch RM, Warren GL, Lowe DA. Estradiol replacement reverses ovariectomy-induced muscle contractile and myosin dysfunction in mature female mice. *J Appl Physiol* (1985) 102: 1387–1393, 2007. doi:10.1152/jappphysiol.01305.2006.
47. Moran AL, Warren GL, Lowe DA. Removal of ovarian hormones from mature mice detrimentally affects muscle contractile function and myosin structural distribution. *J Appl Physiol* (1985) 100: 548–559, 2006. doi:10.1152/jappphysiol.01029.2005.
48. Moran AL, Warren GL, Lowe DA. Soleus and EDL muscle contractility across the lifespan of female C57BL/6 mice. *Exp Gerontol* 40: 966–975, 2005. doi:10.1016/j.exger.2005.09.005.
49. Moreno M, Ordoñez P, Alonso A, Díaz F, Tolivia J, González C. Chronic 17beta-estradiol treatment improves skeletal muscle insulin signaling pathway components in insulin resistance associated with aging. *Age (Dordr)* 32: 1–13, 2010. doi:10.1007/s11357-009-9095-2.

50. **Mu P, Tan Z, Cui Y, Liu H, Xu X, Huang Q, Zeng L, Wang T.** 17 β -Estradiol attenuates diet-induced insulin resistance and glucose intolerance through up-regulation of caveolin-3. *Ir J Med Sci* 180: 221–227, 2011. doi:10.1007/s11845-010-0594-z.
51. **Nelson JF, Felicio LS, Randall PK, Sims C, Finch CE.** A longitudinal study of estrous cyclicity in aging C57BL/6J mice: I. Cycle frequency, length and vaginal cytology. *Biol Reprod* 27: 327–339, 1982. doi:10.1095/biolreprod27.2.327.
52. **Nuedling S, Kahlert S, Loebbert K, Doevendans PA, Meyer R, Vetter H, Grohé C.** 17 Beta-estradiol stimulates expression of endothelial and inducible NO synthase in rat myocardium in-vitro and in-vivo. *Cardiovasc Res* 43: 666–674, 1999. doi:10.1016/S0008-6363(99)00093-0.
53. **Nuedling S, Kahlert S, Loebbert K, Meyer R, Vetter H, Grohé C.** Differential effects of 17beta-estradiol on mitogen-activated protein kinase pathways in rat cardiomyocytes. *FEBS Lett* 454: 271–276, 1999. doi:10.1016/S0014-5793(99)00816-9.
54. **Ogawa S, Chan J, Gustafsson JA, Korach KS, Pfaff DW.** Estrogen increases locomotor activity in mice through estrogen receptor alpha: specificity for the type of activity. *Endocrinology* 144: 230–239, 2003. doi:10.1210/en.2002-220519.
55. **Özdemir Kumral ZN, Kalgazi M, Üstünova S, Kasımay Çakar Ö, Çevik OD, Şener G, Yeğen BC.** Estrogen receptor agonists alleviate cardiac and renal oxidative injury in rats with renovascular hypertension. *Clin Exp Hypertens* 38: 500–509, 2016. doi:10.3109/10641963.2015.1116550.
56. **Phillips SK, Rook KM, Siddle NC, Bruce SA, Woledge RC.** Muscle weakness in women occurs at an earlier age than in men, but strength is preserved by hormone replacement therapy. *Clin Sci (Lond)* 84: 95–98, 1993. doi:10.1042/cs0840095.
57. **Pöllänen E, Kangas R, Horttanainen M, Niskala P, Kaprio J, Butler-Browne G, Mouly V, Sipilä S, Kovanen V.** Intramuscular sex steroid hormones are associated with skeletal muscle strength and power in women with different hormonal status. *Aging Cell* 14: 236–248, 2015. doi:10.1111/accel.12309.
58. **Qaisar R, Renaud G, Hedstrom Y, Pöllänen E, Ronkainen P, Kaprio J, Alen M, Sipilä S, Artemenko K, Bergquist J, Kovanen V, Larsson L.** Hormone replacement therapy improves contractile function and myonuclear organization of single muscle fibres from postmenopausal monozygotic female twin pairs. *J Physiol* 591: 2333–2344, 2013. doi:10.1113/jphysiol.2012.250092.
59. **Ribas V, Drew BG, Zhou Z, Phun J, Kalajian NY, Soleymani T, Daraei P, Widjaja K, Wanagat J, de Aguiar Vallim TQ, Fluit AH, Bensinger S, Le T, Radu C, Whitelegge JP, Beaven SW, Tontonoz P, Lusis AJ, Parks BW, Vergnes L, Reue K, Singh H, Bopassa JC, Toro L, Stefani E, Watt MJ, Schenk S, Akerstrom T, Kelly M, Pedersen BK, Hewitt SC, Korach KS, Hevener AL.** Skeletal muscle action of estrogen receptor α is critical for the maintenance of mitochondrial function and metabolic homeostasis in females. *Sci Transl Med* 8: 334ra54, 2016. doi:10.1126/scitranslmed.aad3815.
60. **Ribas V, Nguyen MT, Henstridge DC, Nguyen AK, Beaven SW, Watt MJ, Hevener AL.** Impaired oxidative metabolism and inflammation are associated with insulin resistance in ERalpha-deficient mice. *Am J Physiol Endocrinol Metab* 298: E304–E319, 2010. doi:10.1152/ajpendo.00504.2009.
61. **Ronda AC, Buitrago C, Boland R.** Role of estrogen receptors, PKC and Src in ERK2 and p38 MAPK signaling triggered by 17 β -estradiol in skeletal muscle cells. *J Steroid Biochem Mol Biol* 122: 287–294, 2010. doi:10.1016/j.jsbmb.2010.05.002.
62. **Ronda AC, Vasconsuelo A, Boland R.** 17 β -estradiol protects mitochondrial functions through extracellular-signal-regulated kinase in C2C12 muscle cells. *Cell Physiol Biochem* 32: 1011–1023, 2013. doi:10.1159/000354502.
63. **Schmidt CA, Ryan TE, Lin CT, Inigo MM, Green TD, Brault JJ, Spangenburg EE, McClung JM.** Diminished force production and mitochondrial respiratory deficits are strain-dependent myopathies of sub-acute limb ischemia. *J Vasc Surg* 65: 1504–1514.e11, 2017. doi:10.1016/j.jvs.2016.04.041.
64. **Skelton DA, Phillips SK, Bruce SA, Naylor CH, Woledge RC.** Hormone replacement therapy increases isometric muscle strength of adductor pollicis in post-menopausal women. *Clin Sci (Lond)* 96: 357–364, 1999. doi:10.1042/cs0960357.
65. **Sotiriadou S, Kyparos A, Albani M, Arsoos G, Clarke MS, Sidiras G, Angelopoulou N, Matziari C.** Soleus muscle force following downhill running in ovariectomized rats treated with estrogen. *Appl Physiol Nutr Metab* 31: 449–459, 2006. doi:10.1139/h06-008.
66. **Torres MJ, Kew KA, Ryan TE, Pennington ER, Lin CT, Buddo KA, Fix AM, Smith CA, Gilliam LA, Karvinen S, Lowe DA, Spangenburg EE, Zeczycki TN, Shaikh SR, Neuffer PD.** 17beta-Estradiol directly lowers mitochondrial membrane microviscosity and improves bioenergetic function in skeletal muscle. *Cell Metab* 27: 167–179.e7, 2018. doi:10.1016/j.cmet.2017.10.003.
67. **Velders M, Solzbacher M, Schleipen B, Laudenbach U, Fritze-meier KH, Diel P.** Estradiol and genistein antagonize the ovariectomy effects on skeletal muscle myosin heavy chain expression via ER-beta mediated pathways. *J Steroid Biochem Mol Biol* 120: 53–59, 2010. doi:10.1016/j.jsbmb.2010.03.059.
68. **Vidal O, Lindberg M, Sävendahl L, Lubahn DB, Ritzen EM, Gustafsson JA, Ohlsson C.** Disproportional body growth in female estrogen receptor-alpha-inactivated mice. *Biochem Biophys Res Commun* 265: 569–571, 1999. doi:10.1006/bbrc.1999.1711.
69. **Warren GL 3rd, Williams JH, Ward CW, Matoba H, Ingalls CP, Hermann KM, Armstrong RB.** Decreased contraction economy in mouse EDL muscle injured by eccentric contractions. *J Appl Physiol* (1985) 81: 2555–2564, 1996. doi:10.1152/jappl.1996.81.6.2555.
70. **Weigt C, Hertrampf T, Kluxen FM, Flenker U, Hülsemann F, Fritze-meier KH, Diel P.** Molecular effects of ER alpha- and beta-selective agonists on regulation of energy homeostasis in obese female Wistar rats. *Mol Cell Endocrinol* 377: 147–158, 2013. doi:10.1016/j.mce.2013.07.007.
71. **Zhai P, Eurell TE, Cooke PS, Lubahn DB, Gross DR.** Myocardial ischemia-reperfusion injury in estrogen receptor-alpha knockout and wild-type mice. *Am J Physiol Heart Circ Physiol* 278: H1640–H1647, 2000. doi:10.1152/ajpheart.2000.278.5.H1640.